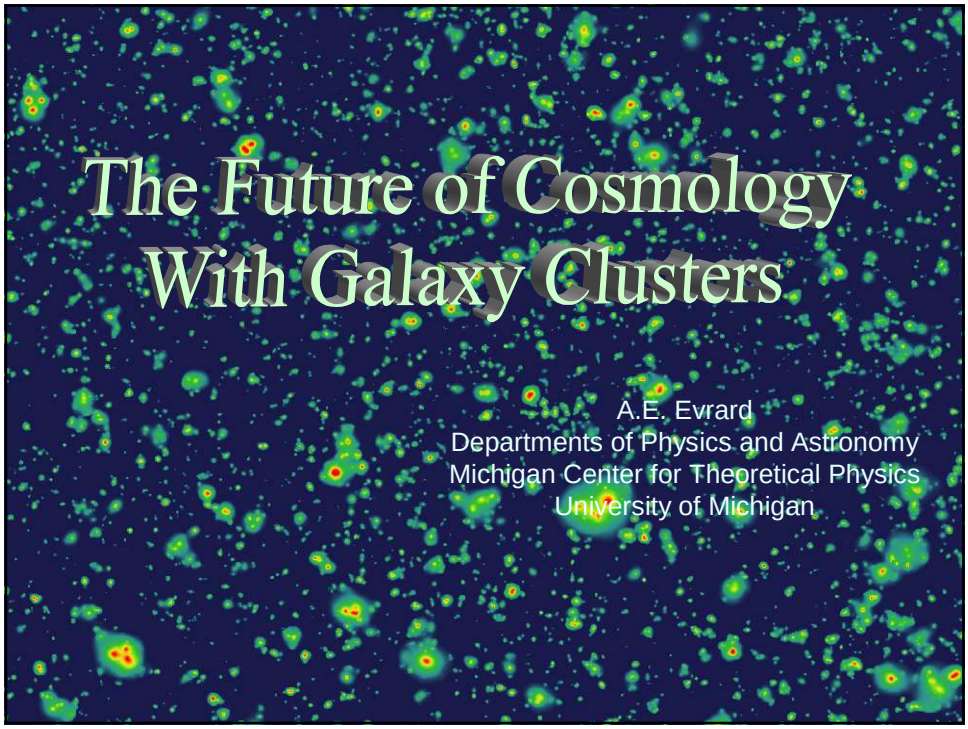

early `large' surveys: clusters= largest, grav. bound systems

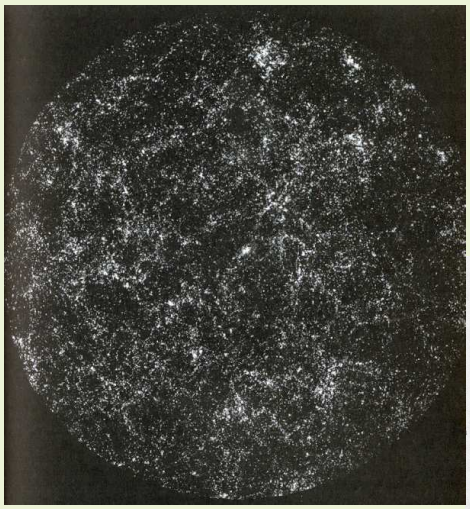

Lick catalog of
400,000 galaxies

Shane & Wirtanen 1967

Seldner et al. 1977

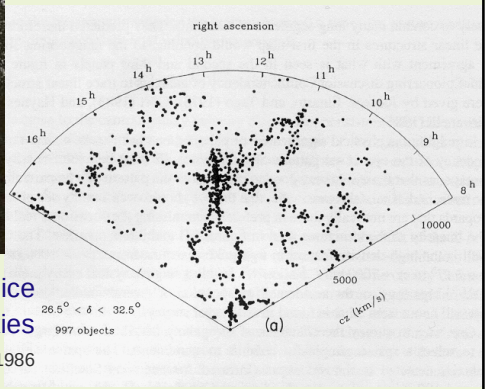

CfA catalog 6 deg slice
~1,000 galaxies

deLapparent, Geller & Huchra 1986

clusters are the `birthplace' of dark matter

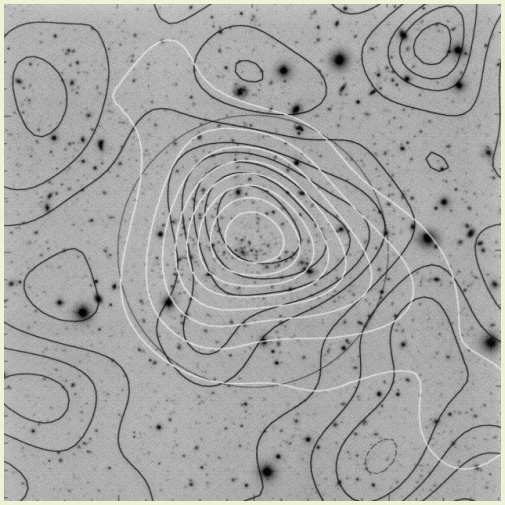

MS1054: Luppino & Kaiser 1997

Fritz Zwicky

virial equilibrium of galaxies (1933)

$$M = c\,\sigma_{gal}^{2}\,\langle r_{gal}\rangle / G$$

weak gravitational lensing (1997)

$$M = \kappa\,\Sigma_{crit}\,\Delta\Omega$$

strong lensing cluster cores are natural telescopes

Kneib et al. 2004

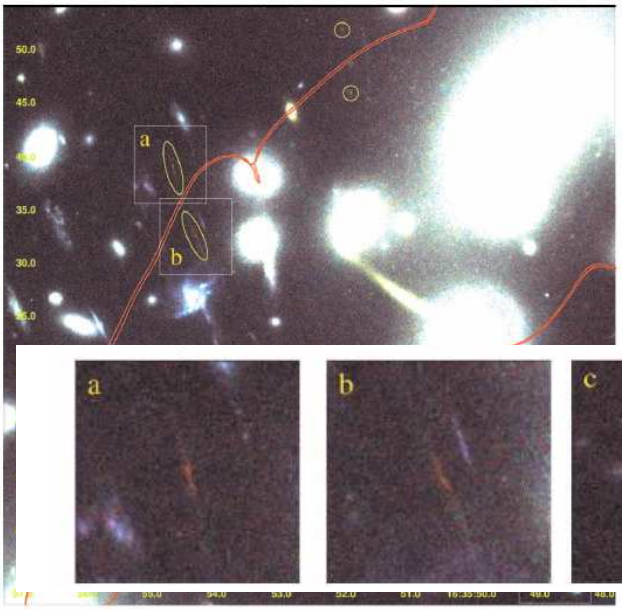

triply imaged galaxy in A2218

~25x mag

$z \sim 7$

$r \sim 1$ kpc

$dM_{star}/dt \sim 2.5$

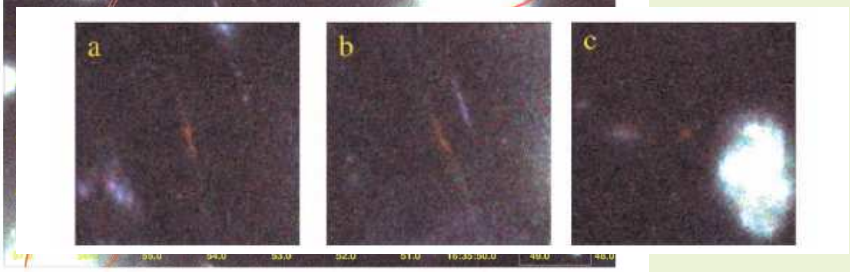

clusters' deep potential wells trap `missing' baryons

optical

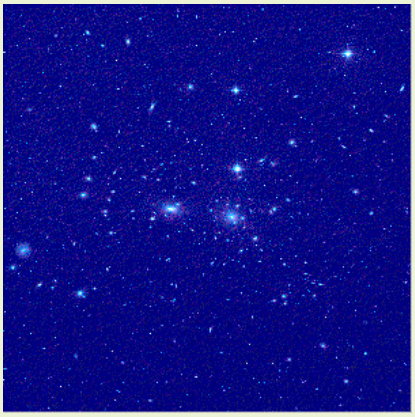

X-ray

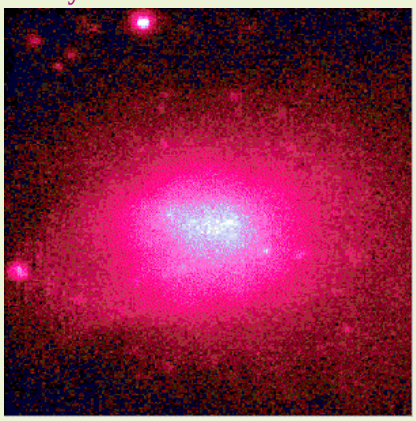

$$M_{\rm gal} = 1.0 \pm 0.2 \times 10^{13} h^{-1} M_{\Theta}$$

$$M_{\rm ICM} = 5.5 \pm 1.0 \times 10^{13} h^{-5/2} M_{\Theta}$$

hot intracluster medium (ICM) dominates visible mass

$M_{ICM} \sim 10\ (h/0.65)^{-3/2}\ M_{gal}$

estimates for Coma

White et al 1993

Chandra/XMM offer increasing detailed views of hot ICM

Henry et al 2004

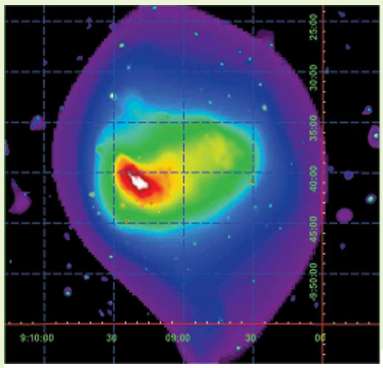

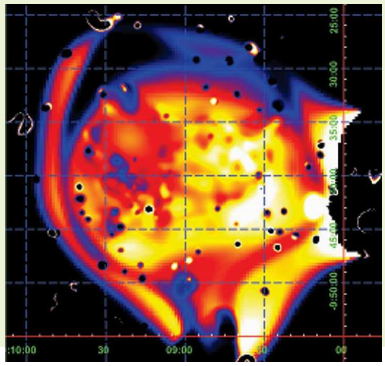

September 28, 2004

New York Times

When Clusters Collide

By HENRY FOUNTAIN

As collisions go, the one taking place in the vicinity of the constellation Hydra is a doozy. Out there, some 800 million light-years from Earth, two galactic clusters - one with about 1,000 galaxies, the other with 300, totaling trillions of stars - have gone bump in the night.

Astronomers have released the clearest picture yet of this collision, one of the most energetic events in the universe after the Big Bang. Data from the XMM-Newton satellite, an X-ray observatory operated by the

clusters surveys: many efforts in different wavebands

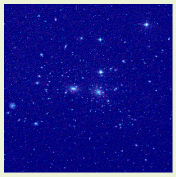

SDSS
N~10^4 to z~0.6

RCSII
N~10^4 to z~1.4

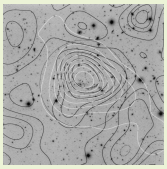

DLS
N~10^2 to z~1

SNAP?
N~10^4 to z~2?

REFLEX/NORAS
N~10^3 to z~0.5

MACS
N~10^2 to z~1

XCS
N~10^4 to z~1.5

DUO (phase A SMEX)
N~10^4 to z~1.5

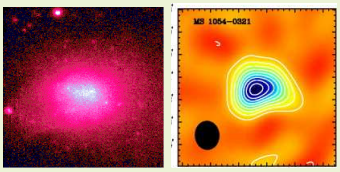

APEX-SZ
N~10^3 to z~3

SZA
N~10^3 to z~3

AMI
N~10^3 to z~3

SPT
N~10^4 to z~2

cluster tests of dark energy

Friedmann equation

$$H^2(z) = H_0^2 \left[\Omega_m (1+z)^3 + \Omega_X (1+z)^{3(1+w)}\right]$$

controls distance/volume as function of redshift

$$r(z) = \int_0^z \frac{dz'}{H(z')}$$

and growth rate of linear perturbations

$$\ddot{\delta} + 2H\dot{\delta} - 4\pi G \rho_m \delta = 0$$

<u>Phenomenology:</u>

number counts: N(M,z)

clustering: $\xi(r \mid M,z)$; counts in cells

characteristic sizes: f_{gas} ; angular sizes

tests of dark energy: counts

Haiman, Mohr & Holder 2001

mass limited sample $>10^{14}$ M_{sun}

- ΛCDM
- $w = -0.6$
- $w = -0.2$
- OCDM

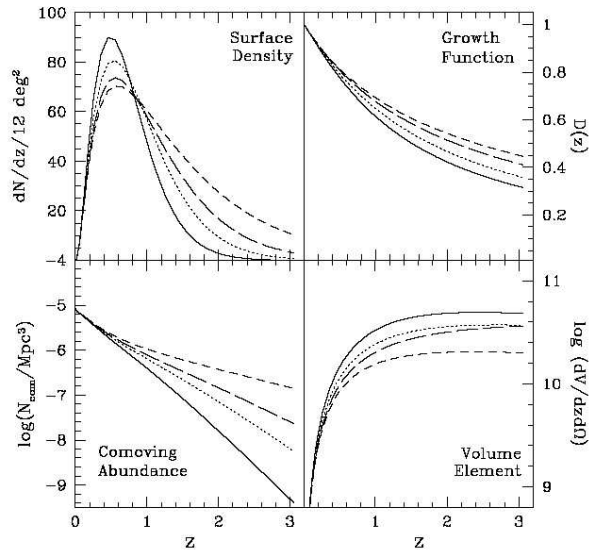

FIG. 3.—Effect of changing w when all other parameters are held fixed. The solid curve shows our fiducial flat ΛCDM model, with $w = -1$, $\Omega_m = 0.3$, and $h = 0.65$. The dotted curve is the same model with $w = -0.6$, the short-dashed curve with $w = -0.2$, and the long-dashed curve is an open CDM model with $\Omega_m = 0.3$.

dN/dz for SPT 4000 sq degree Survey (could be done in one austral winter)

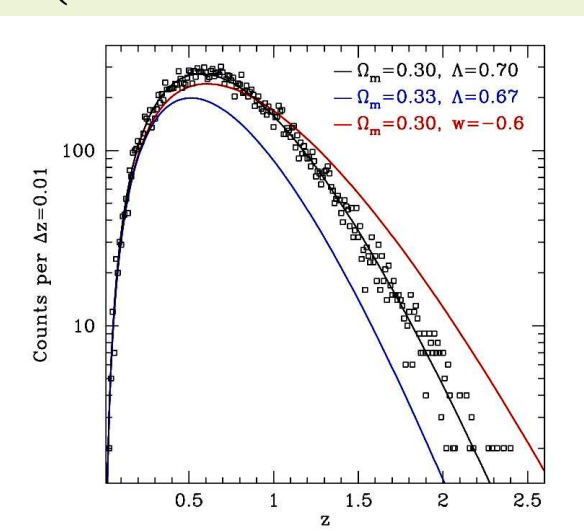

Goal: constrain DE equation of state

$p = w\,\rho$

Courtesy J. Carlstrom (U Chicago)

tests of dark energy: astrophysical confusion

mass limited sample

$>10^{14}$ M_{sun}

Haiman, Mohr & Holder 2001

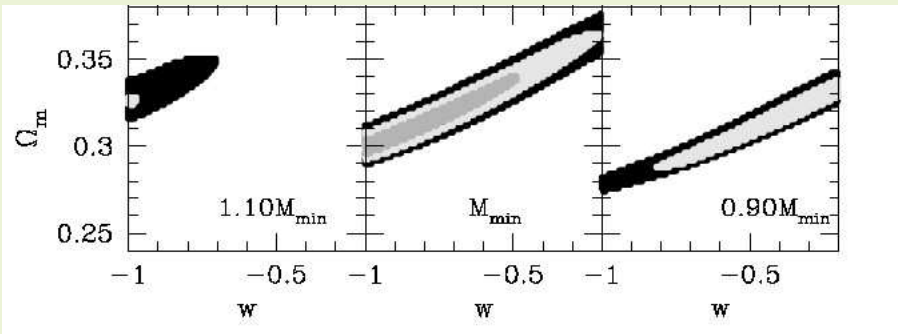

sharpening tools of the cluster trade…

– forged by computational modeling of non-linear structure

– core element is the *mass* of collapsed, quasi-equilibrium regions (halos)

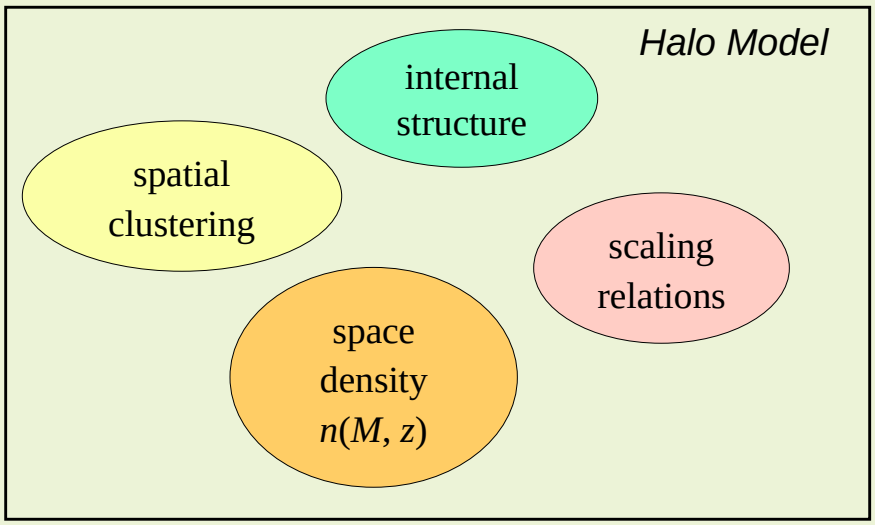

large-scale structure formation via gravitational instability

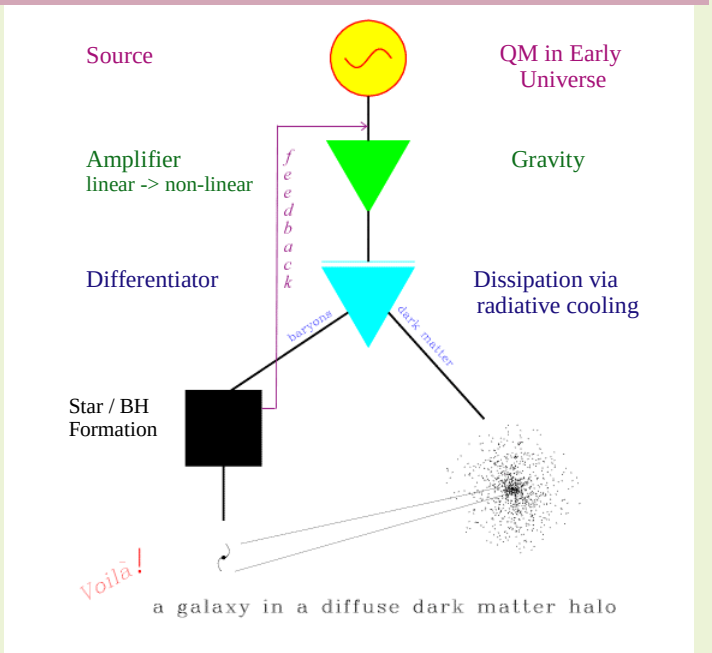

birth of a virtual cluster (physical frame)

B. Moore, http://www.nbody.net

Galaxy Cluster =
"A large knot of quasi-equilibrium, self-gravitating matter embedded within an evolving filamentary network (the `cosmic web') of growing density perturbations."

QuickTime™ and a YUV420 codec decompressor are needed to see this picture.

typical characteristics -

$N_{gal} \sim 10$ or more

$k_B T_X \sim 1\text{-}15$ keV

$R \sim 0.3\text{-}2\ h^{-1}$ Mpc

$M \sim 10^{13} - 10^{15.5}\ h^{-1}\ M_{sun}$

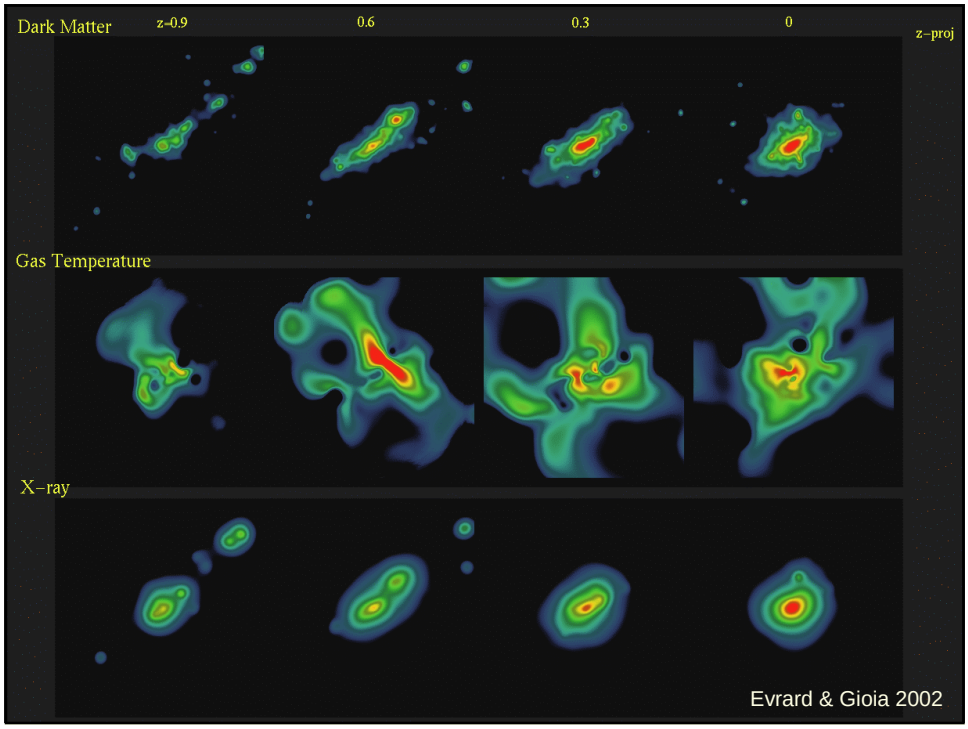
Dark Matter
z=0.9
0.6
0.3
0
z−proj
Gas Temperature
X−ray
Evrard & Gioia 2002

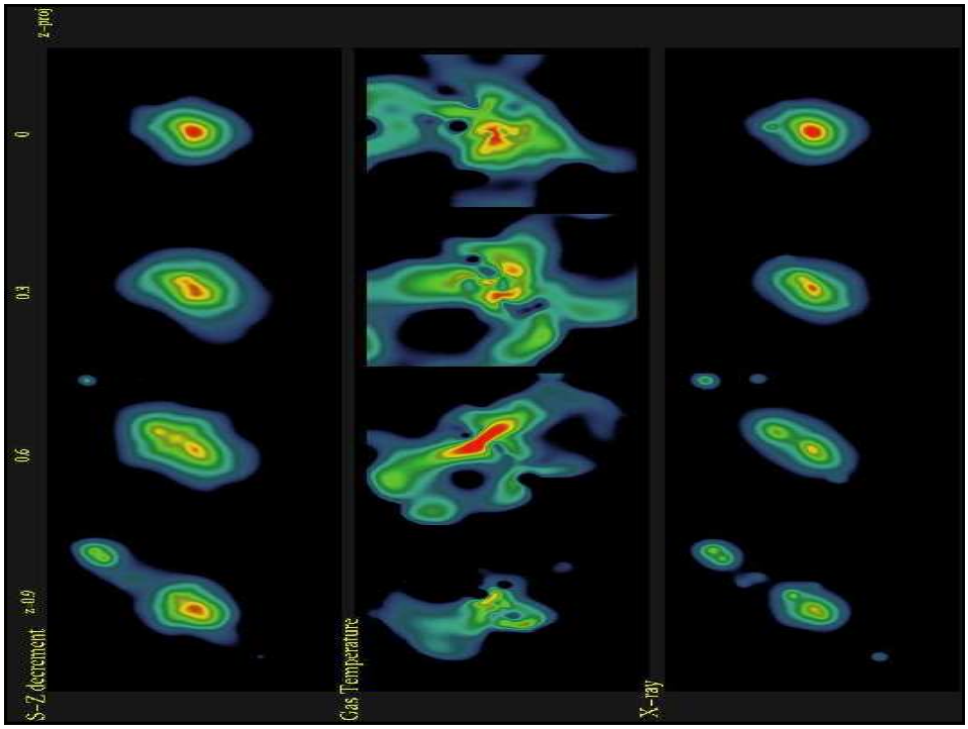
S−Z decrement
z=0.9
0.6
0.3
0
z−proj
Gas Temperature
X−ray

Santa Barbara cluster simulations: radial structure

Frenk et al 1999

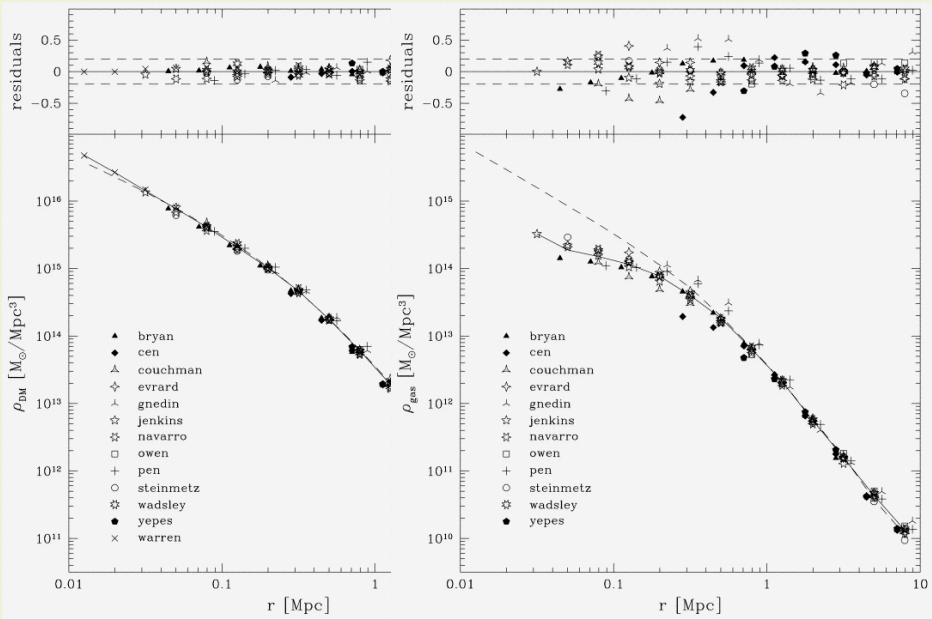

Santa Barbara cluster simulations: bulk measures

Frenk et al 1999

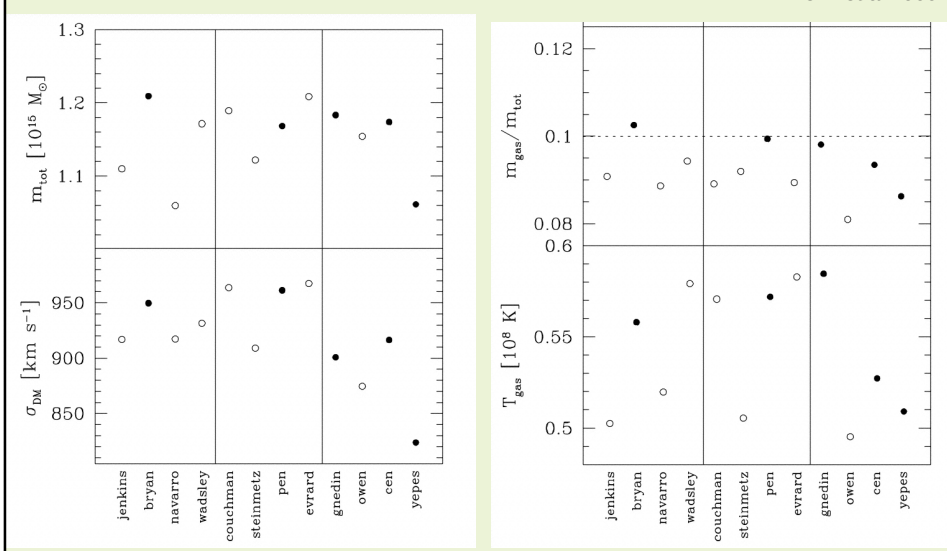

constraints from a constant gas fraction assumption

Allen et al 2004

26 luminous, `dynamically relaxed' clusters observed by Chandra

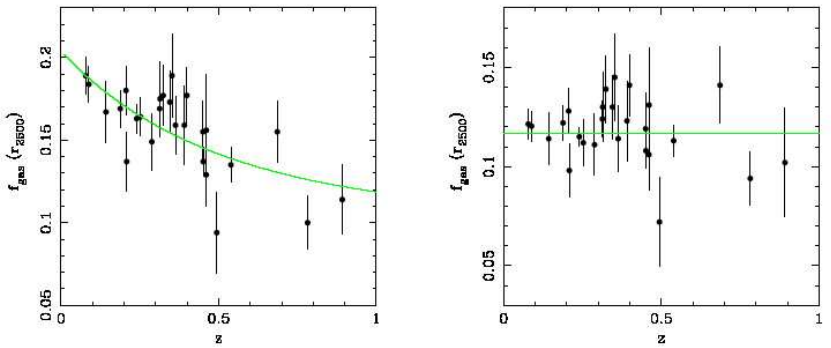

Figure 2. The apparent variation of the X-ray gas mass fraction (with root-mean-square 1σ errors) as a function of redshift for the reference (a: left panel) SCDM and (b: right panel) ΛCDM cosmologies. The grey curve in (a) shows the predicted $f_{gas}(z)$ behaviour for the best-fitting model cosmology with $\Omega_m = 0.25$ and $\Omega_\Lambda = 0.96$ (see Section 3.2). Clusters at higher redshifts appear to have lower gas mass fractions because the SCDM cosmology underestimates the relative distances to these systems. The curve in (b) shows the best-fitting constant value.

constraints from a constant gas fraction assumption

Allen et al 2004

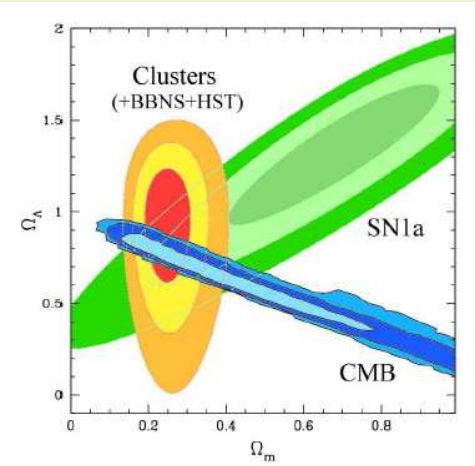

Figure 4. The 68.3, 95.4 and 99.7 per cent (1, 2 and 3σ) confidence constraints in the Ω_m, Ω_Λ plane obtained from the analysis of the cluster f_{gas} data using standard priors on $\Omega_b h^2$ (Kirkman *et al.* 2003) and h (Freedman *et al.* 2001). Also shown are the independent results obtained from CMB data using a weak uniform prior on h ($0.3 < h < 1$), and Type 1a supernovae data (Tonry *et al.* 2003). A ΛCDM cosmology is assumed with the curvature, Ω_K, included as a free parameter in the analysis.

reference point: spherical self-similar infall

Bertschinger 1985

collisionless (DM) infall onto point perturbation in an otherwise `empty' Einstein-deSitter universe

$\lambda = r/r_{ta}$ $\quad r_{ta} \sim t^{8/9}$ $\quad \xi \sim t^{2/3}$

- phase wrapped orbits
- hydrostatic within λ~1/3 `boundary'

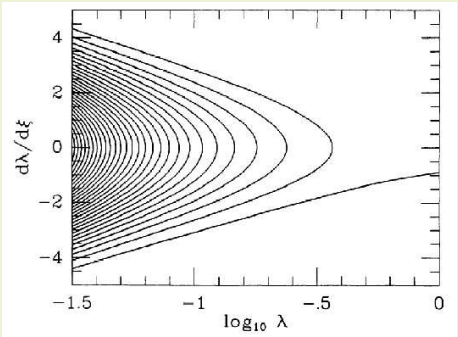

infall of γ= 5/3 gas
- develops shock at λ~1/3
  same `boundary' as dark matter
- hydrostatic interior
- inner gas density profile traces DM
  (except for caustics)

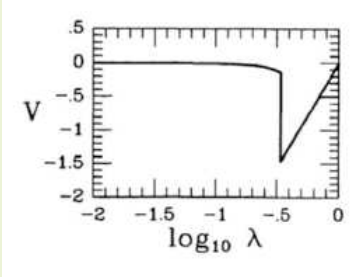

clusters as spherical cows…

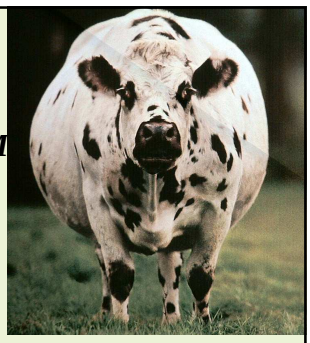

`surface' radius r_Δ & enclosed mass $M_\Delta \equiv M$

$$\rho(< r_\Delta) \equiv 3M_\Delta / 4\pi r_\Delta^{\,3}$$

WARNING! *multiple conventions in literature !*

1. critical contrast $\quad \rho(< r_\Delta) \equiv \Delta\rho_c(z) \;\; ; \;\; \rho_c(z) \equiv 3H(z)^2/8\pi G$

   1a. fixed Δ $\quad \Delta = const \approx 10^2$

   1b. variable Δ: $\quad \Delta(\Omega_m) = 18\pi^2 + 82x - 39x^2 \;\; ; \;\; x \equiv \Omega_m(z) - 1$

2. mean contrast $\quad \rho(< r_\Delta) \equiv \Delta\bar{\rho}_m(z) \;\; ; \;\; \bar{\rho}_m(z) = \Omega_m(z)\rho_c(z)$

Gunn & Gott 1972 ; Bertschinger 1985
Evrard, Metzler & Navarro 1996

spherical cows? where's the hide?

M. White 2002

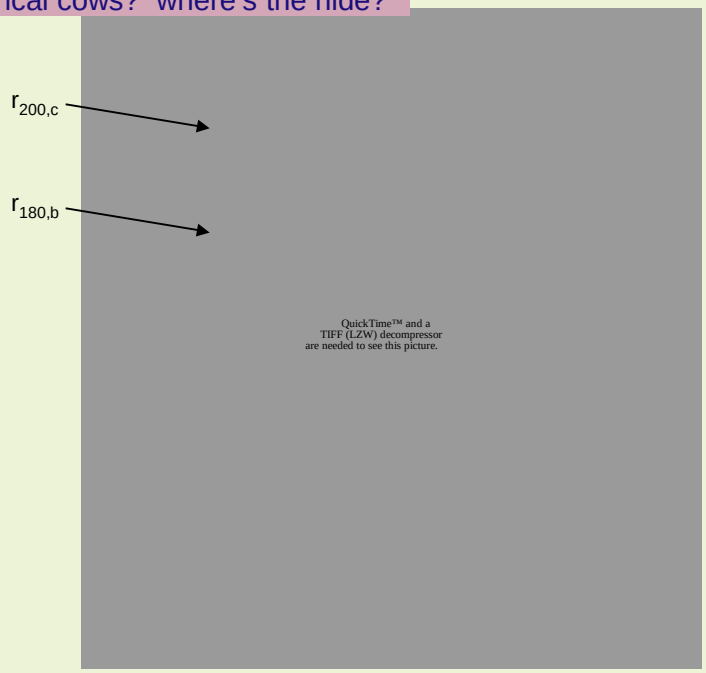

phase-space structure in concordance future

Busha et al, in prep

256^3-particle Gadget model ; Ω_m= 0.3, Ω_Λ= 0.7 ; evolved to 70Gyr (a=100)

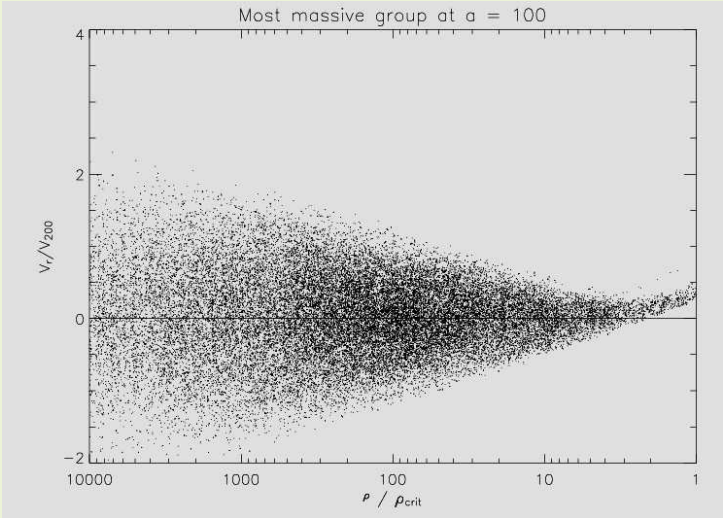

phase-space structure in concordance future

Busha et al, in prep

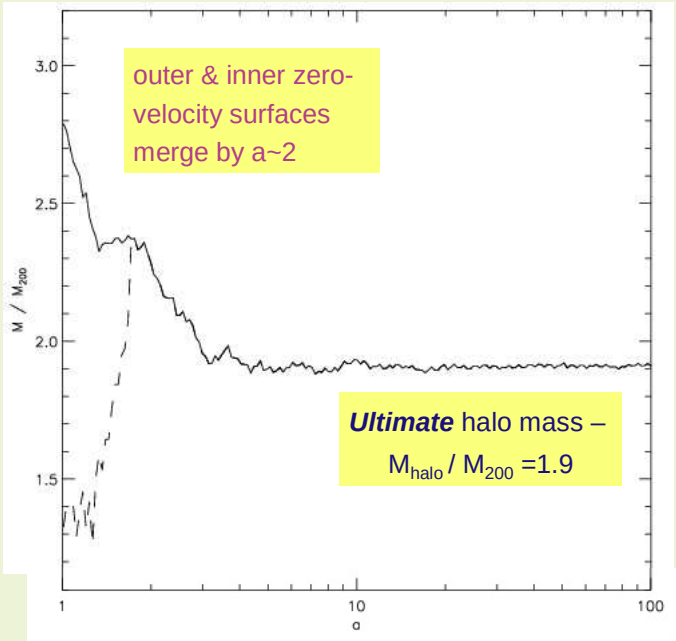

- internal structure -

internal structure of dark matter halos

Navarro, Frenk & White 1996; 97

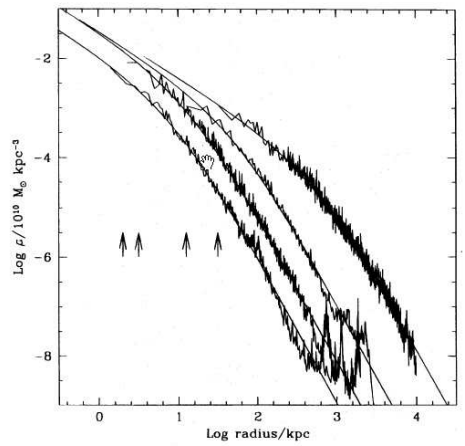

FIG. 3.—Density profiles of four halos spanning 4 orders of magnitude in mass. The arrows indicate the gravitational softening, h_g, of each simulation. Also shown are fits from eq. (3). The fits are good over two decades in radius, approximately from h_g out to the virial radius of each system.

density profiles at z=0 of halos spanning four orders of magnitude in mass M_{200}

fit by single functional form: the `NFW profile'

$$\rho(r) = \frac{\delta_s}{(r/r_s)(1+r/r_s)^2}$$

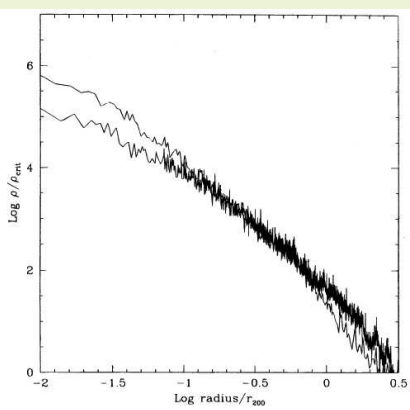

FIG. 4.—Scaled density profiles of the most and least massive halos shown in Fig. 3. The large halo is less centrally concentrated than the less massive system.

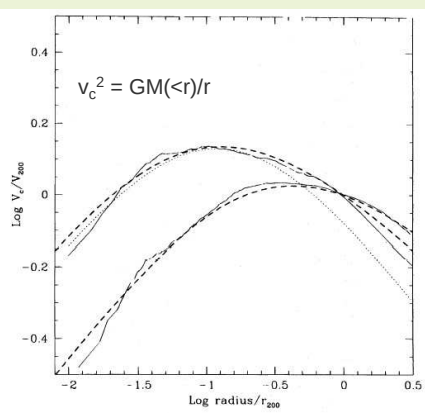

FIG. 6.—Scaled circular velocity profiles of two halos, one of the largest and one of the smallest in our sample (*solid curves*). The dashed lines are fits with eq. (5). The dotted line is a fit to the low-mass system using a Hernquist model (see eq. [6]). Note that the Hernquist model underestimates the halo circular velocity at r_{200}.

Navarro, Frenk & White 1996

halo structure: systematic trends + scatter

Jing & Suto 2000

concentration

$c = r_\Delta / r_s$

simulations show weak trend in c with mass, with significant scatter

not all profiles are well fit due to presence of sub-structure in ongoing mergers

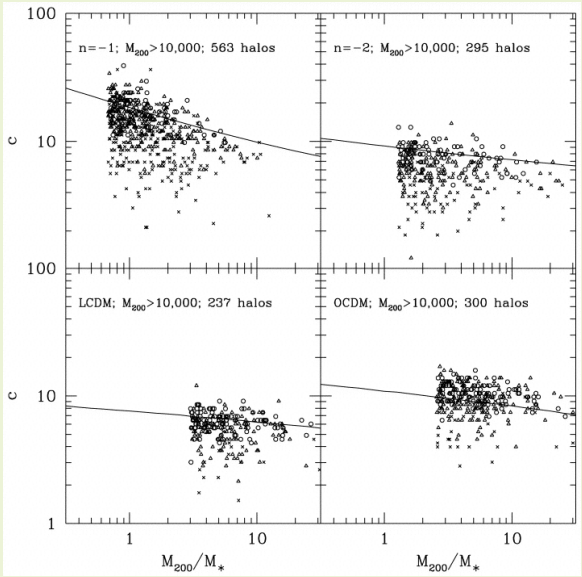

projected radial profiles of 2MASS galaxies

Lin, Mohr, & Stanford 2004

radial profile fits projected NFW form with c=3.0±0.3

real data!

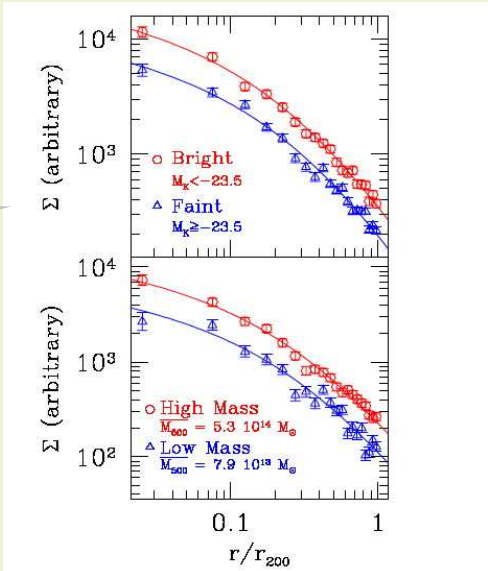

FIG. 8.— *Top:* Comparison of profiles for galaxies brighter and fainter than $M_K = -23.5$ in all clusters. The best-fit profiles have $c_g = 3.0 \pm 0.3$ (bright) & 2.8 ± 0.3 (faint). *Bottom:* Galaxy distribution in the most and least massive 25 clusters (the mean masses are

concentration is linked to formation history

Wechsler et al 2002
Bullock et al 2001

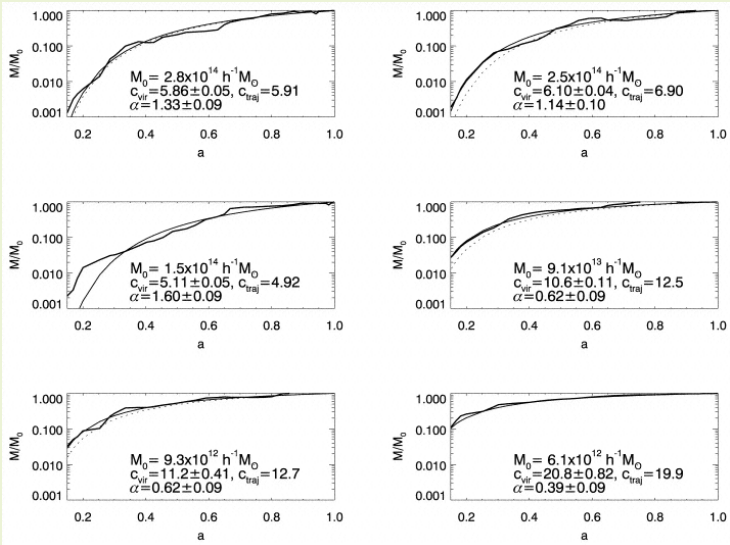

$$M_{\max}(a) = M_0 \exp[-a_c S(a_o/a - 1)] \;\; ; \;\; (S = 2)$$

internal structure of dark matter halos

Wechsler et al 2002

early formation ↔ high c
late formation ↔ low c

possible avenue to constraining dark energy models, but effects are small and degenerate with σ_8.

Dolag et al 2004

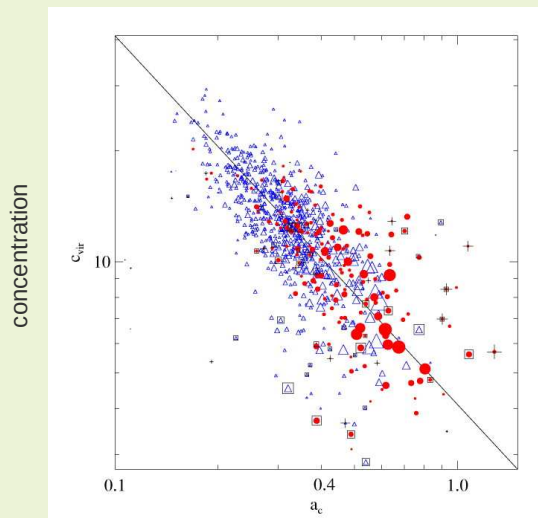

formation epoch

- space density -

space density (aka, ***mass function***) takes `universal' form in σ(M)

$$n(\sigma^{-1}(M)) \propto A(\rho_{\mathrm{m}}/M)\exp[-|\ln\sigma^{-1}(M)+B|^{\varepsilon}]$$

Jenkins et al 2001
Sheth & Tormen 1999

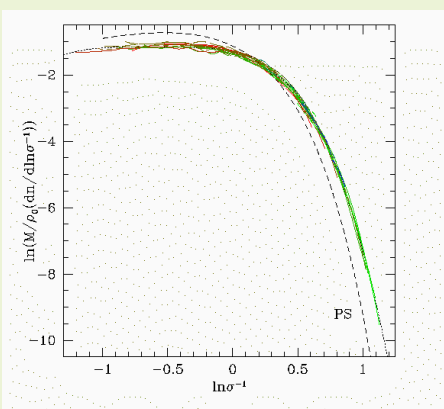

Figure 7. The FOF(0.2) mass functions of all the simulation outputs listed in Table 2. Remarkably, when a single linking length is used to identify halos at all times and in all cosmologies, the mass function appears to be invariant in the $f - \ln\sigma^{-1}$ plane. A single formula (eqn. 9), shown with a dotted line, fits all the mass functions with an accuracy of better than about 20% over the entire range. The dashed curve show the Press-Schechter mass function for comparison.

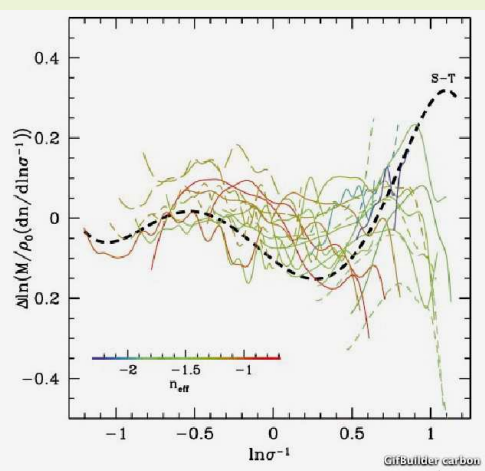

critical Δ=200 mass function calibration from Hubble Volume sims

Evrard et al 2002

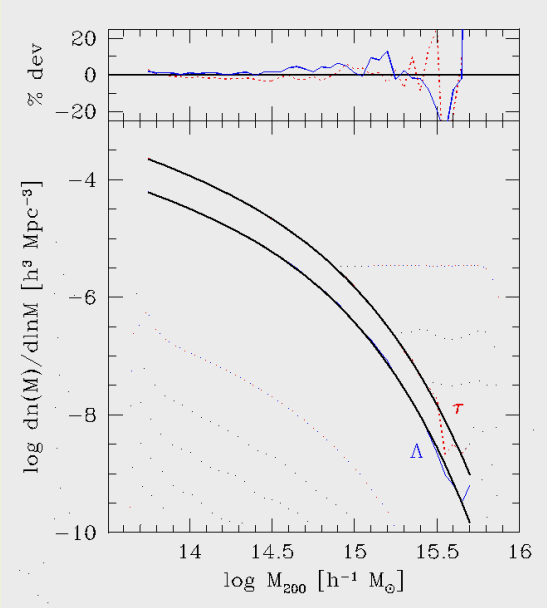

<- rms deviations about fit at <~5% level

fit to functional form of Jenkins et al 2001 using ~1.4M clusters at z=0

fit parameters A, B are now Ω_m dependent

Hu & Kratsov `02 - ART simulation

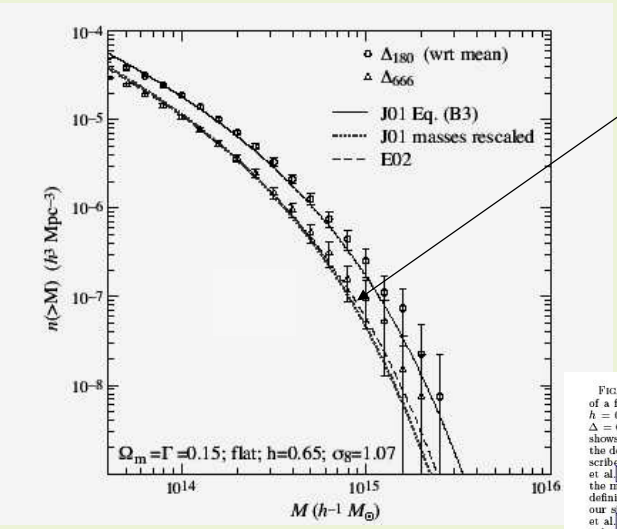

uses parameters fit as linear ftn's of Ω_m

calibrated@ Ω_m=0.3

applied@ Ω_m=0.15

FIG. B10.— Cluster mass functions derived from the simulation of a flat low-Ω_m CDM cosmology ($\Omega_m = 1 - \Omega_{DE} = \Gamma = 0.15$; $h = 0.65$; $n_s = 1$; $\sigma_8 = 1.07$) using masses defined by Δ_{180} and $\Delta = 666.6$. The error bars show 2σ Poisson errors. The *solid line* shows the fit obtained by Jenkins et al (2001, their Eqn. B3) while the dotted line shows this fit with M_{180} converted to M_{666} as described in the Appendix C. Agreement indicates that the Jenkins et al fit should be interpreted as M_{180}, defined with respect to the mean density and that the mass function is universal for this definition of mass. The converted mass function fit matches both our simulated mass function for $\Delta = 666$ and the fit of Evrard et al (2002, their Tab. 1) to the mass function from the Hubble volume ΛCDM simulation with this definition of mass. The agreement shows that conversion assuming an NFW profile adequately accounts for the substantial differences between M_{180} and M_{666}.

observed space density in X-rays

Mullis et al 2004

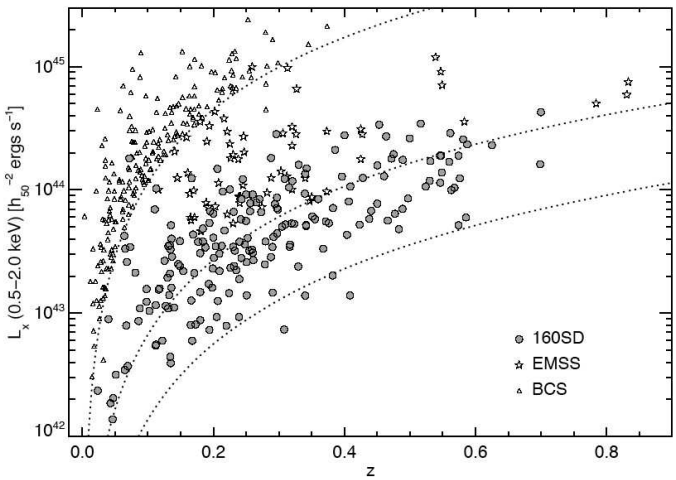

FIG. 1.— X-ray luminosity and redshift distribution of the 160SD (Mullis et al. 2003), the EMSS (Gioia & Luppino 1994 with updates from the literature, e.g., Henry 2000), and the BCS (Ebeling et al. 1998) cluster samples. The dotted curves (left to right) are indicative flux limits of 2.7×10^{-12}, 1.5×10^{-13}, and 3×10^{-14} ergs cm^{-2} s^{-1} (0.5–2.0 keV). The EMSS and BCS luminosities were converted to this energy band assuming a Raymond-Smith plasma spectrum (Raymond & Smith 1977) with a metallicity of 0.3 solar and the reported gas temperature (either directly measured or estimated from the luminosity-temperature relation).

observed space density in X-rays

Mullis et al 2004

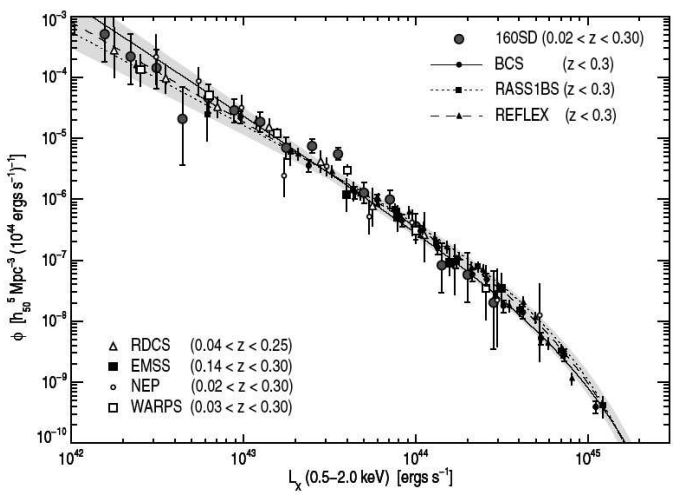

FIG. 5.— Compilation of local XLFs as measured by eight X-ray flux-limited surveys. RDCS: Rosati et al. (1998), EMSS: Henry et al. (1992), NEP: Gioia et al. (2001), and WARPS: Jones et al. (2000b) and the references in Figure 4 (Einstein–de-Sitter universe).

- clustering -

clustering: massive halos are `positively biased'

Mo & White 1996
Sheth, Mo & Tormen 2000

halo 2-pt correlation function (or power spectrum) is biased version of overall matter 2-pt ftn

$$\xi_h(r;M) = b^2(M)\xi(r),$$

where

$$b(M) = 1 + \frac{\delta_c}{\sigma^2(M)} - \frac{1}{\delta_c}.$$

$$\sigma^2(M) = \int d^3k W(kM^{1/3}) P(k)$$

for power-law $P(k) \sim k^n$
$\sigma \sim M^{-(n+3)/6}$

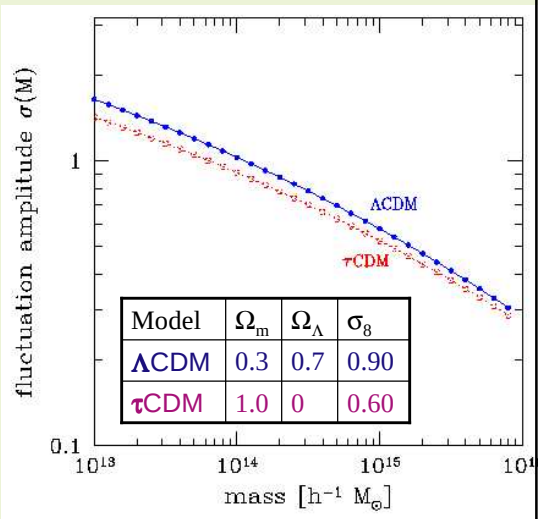

Model	Ω_m	Ω_Λ	σ_8
ΛCDM	0.3	0.7	0.90
τCDM	1.0	0	0.60

halo bias from Hubble Volume simulations

Colberg et al 2000

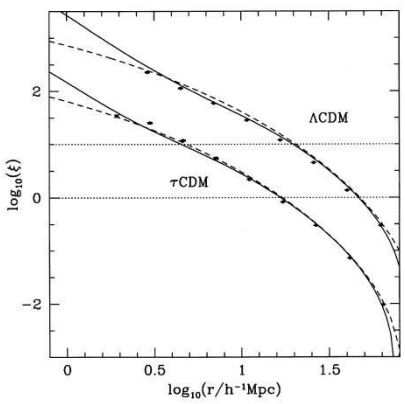

Figure 2. The two-point correlation functions of the τCDM (lower plots) and ΛCDM (upper plots) models for $d_c = 50h^{-1}$ Mpc. This figure compares results from the simulations (dots with error bars) with the linear (dashed line) and non-linear (solid line) predictions from equation (2) with the SMT prediction for b. For the ΛCDM model all quantities have been shifted upwards by one order of magnitude. 1σ error bars are plotted, as in Fig. 1.

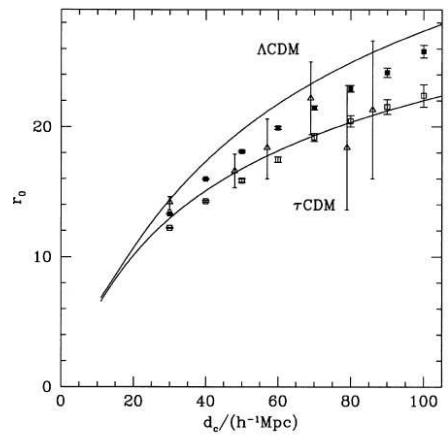

Figure 3. Correlation length, r_0, as a function of mean intercluster separation, d_c, for the τCDM (open squares) and ΛCDM (filled squares) simulations. The predictions of the SMT model are shown as solid lines. Also shown are data from the APM cluster catalogue (open triangles), taken from Croft et al. (1997).

halo bias from HOT simulations

Seljak & Warren 2004

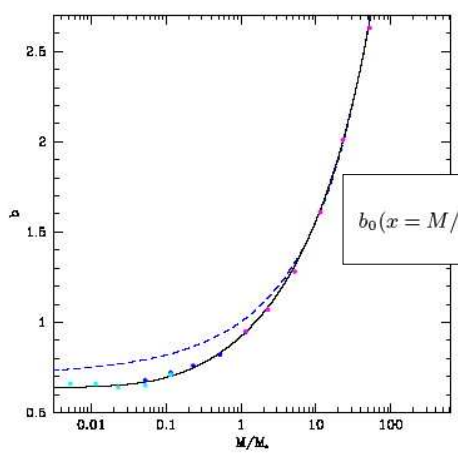

$$b_0(x = M/M_{\rm nl}) = 0.53 + 0.39x^{0.42} + \frac{0.08}{40x+1} + 10^{-4}x^{1.7}.$$

Figure 7. Bias as a function of mass in units of the nonlinear mass. Points are from HOT1 (lowest masses), HOT2 (intermediate masses) and HOT3 (highest masses) simulations. We only show HOT1-3, but we have several other simulations of this model which agree with these results. Note that in a few cases the points from two simulations overlap exactly. Upper (dashed blue) line is theoretical prediction from Sheth and Tormen (1999). Lower (solid black) line is the expression from equation 5.

observed bias in X-ray selected REFLEX sample

Schuecker et al 2001

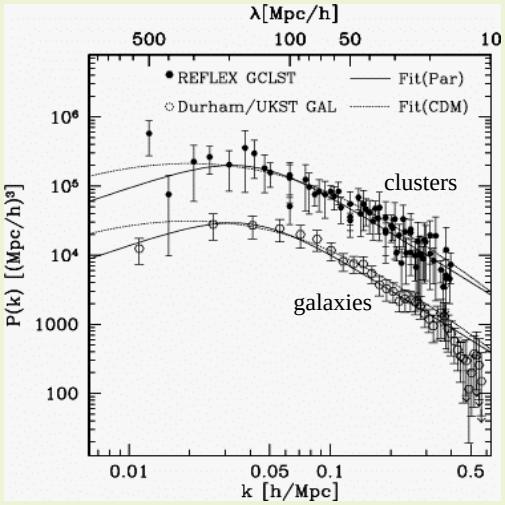

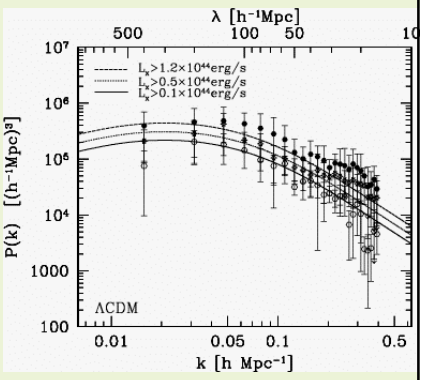

observed bias in 2dFGRS groups

Yang et al 2004

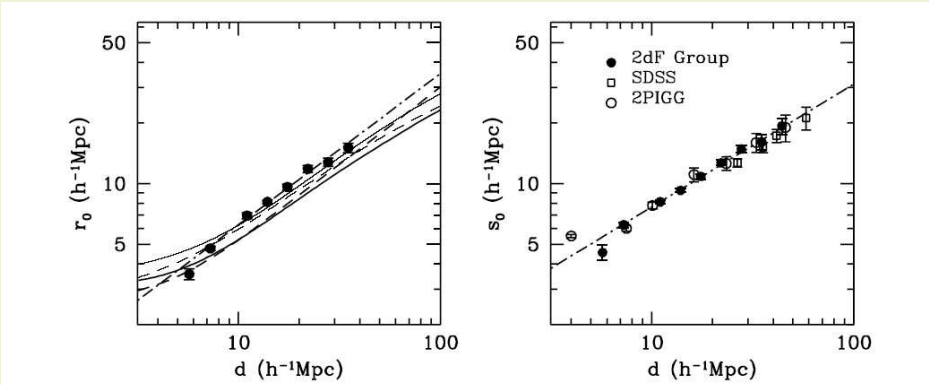

Figure 5. *Left panel:* The relation between r_0 and d for groups selected from the 2dFGRS (solid dots). Errorbars indicate the 1-σ variance from 8 independent mock group samples. The solid and dashed lines are model predictions for a ΛCDM cosmology with $\sigma_8 = 0.9$ and 0.7, respectively. Thick and thin lines are based on the bias models of SW04 and SMT01, respectively. The dot-dashed line, finally, corresponds to the best-fit power-law relation, $r_0 = 1.11\,d^{0.75}$. *Right panel:* The relation between the redshift-space correlation length, s_0, and mean group separation, d, for our 2dFGRS group catalogue (solid dots), compared to those of the SDSS (Bahcall et al. 2003) and 2PIGG (Padilla et al. 2004). The dot-dashed line corresponds to the best-fit power-law, $s_0 = 1.88\,d^{0.61}$.

- scaling relations -

virial scaling between mass and temperature

links total mass to direct observables (gas T & galaxy velocities)

$$\sigma^2 \approx \frac{kT_X}{\mu m_p} \propto \frac{GM_\Delta}{r_\Delta}$$

for mass defined within a *critical* density threshold Δ, expect self-similar clusters (fixed concentration c_{NFW}) to follow

$$H(z)M_\Delta = A_T(c_{\mathrm{NFW}})T^{3/2} = A_\sigma(c_{\mathrm{NFW}})\sigma^3$$

ICM virial relation: computational calibration

Mathiesen & Evrard `01
48 P3MSPH simulations

T alone is a low-noise mass estimator:
~11 % scatter in $h(z)M_{500}$ at fixed *kT*

power-law fit parameters are independent of cosmology/epoch

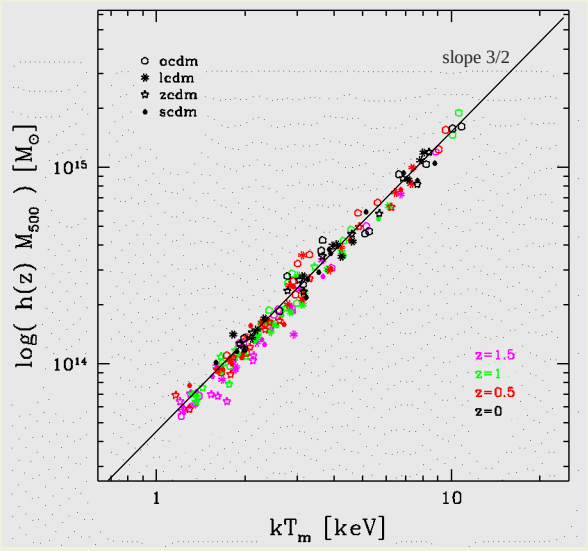

DM virial relation: a "world" calibration

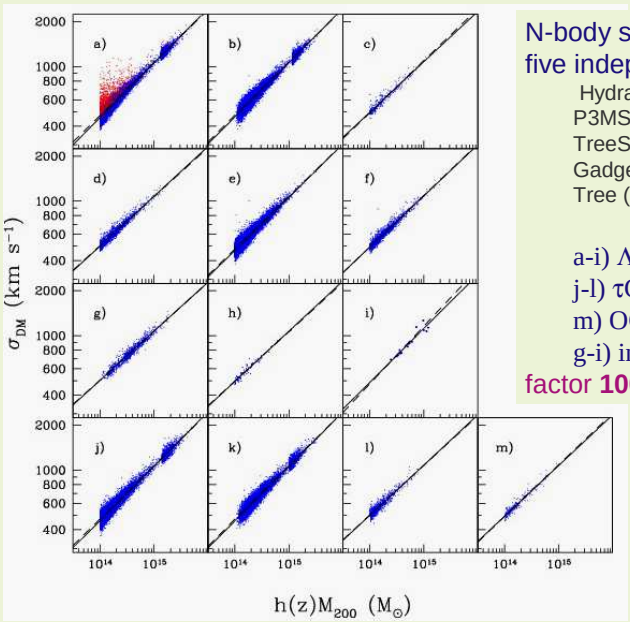

N-body simulation data from five independent groups
- Hydra (Jenkins, Couchman)
- P3MSPH (Evrard, Bialek)
- TreeSPH (M. White)
- Gadget (Springel, Tormen)
- Tree (Warren, Heitmann, Habib)

a-i) ΛCDM
j-l) τCDM
m) OCDM
g-i) include 10% gas

factor **1000** in mass resolution

DMVT "world" calibration: percent calibration of intercept $\sigma_{DM,15}$

$$\sigma_{DM}(\ldots\ I_{sun}]^{\alpha}$$

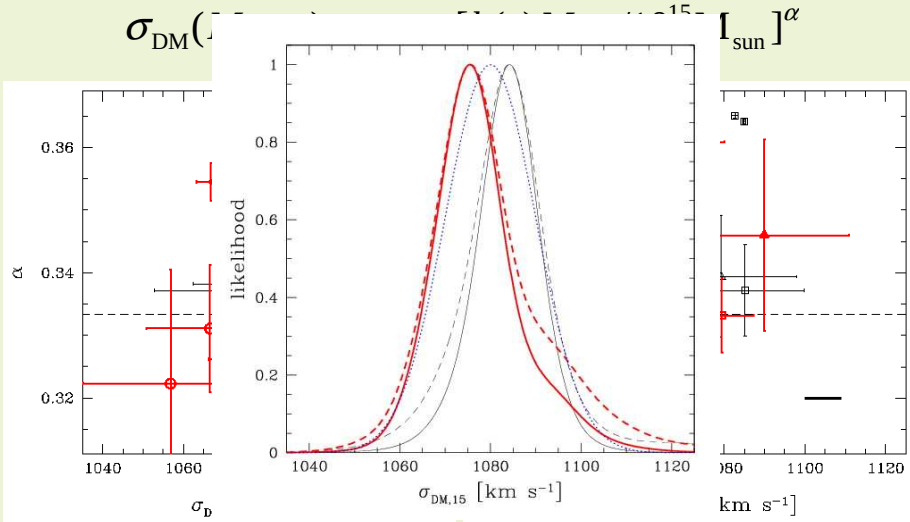

$$\sigma_{DM,15} = 1080 \pm 10 \text{ km s}^{-1}$$

from dark to light: matching the observed space density $n(T_X)$

$$n(M) \xrightarrow{\text{V.Th}^{m}} n(\sigma_{DM}) \xrightarrow{\beta} n(T_X)$$

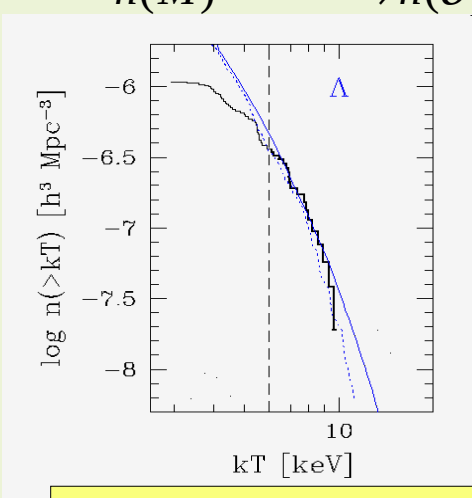

ratio of specific energies

$$\beta = \sigma_{DM}^{2} / (kT_X / \mu m_p)$$

to match observed n(T): degeneracy between ICM thermal physics & power spectrum normalization

best fit:

$$\beta\ \sigma_8^{-5/3} = 1.10 \pm 0.07$$

$$hM_{500}^{tot}(6\text{ keV}) = (0.64 \pm .06)\sigma_8^{5/2} \times 10^{15} M_o$$

Evrard et al 2002
Huterer & White 2002

ICM mass-temperature relation for X-ray flux-limited sample

Mohr, Mathiesen & Evrard 99

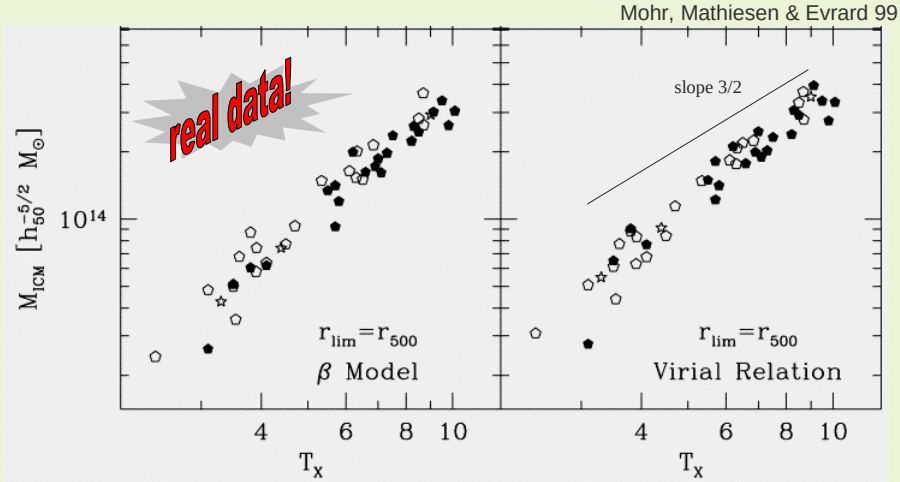

14 % scatter in M_{ICM} at fixed T_X

X-ray luminosity-temperature relation requires complex ICM

Arnaud & Evrard 1999

self-similar model: purely gravitational heating + constant ICM gas fraction

extra physics?
- gas cooling
- gas heating from winds/AGN
- other `ISM-like' processes?

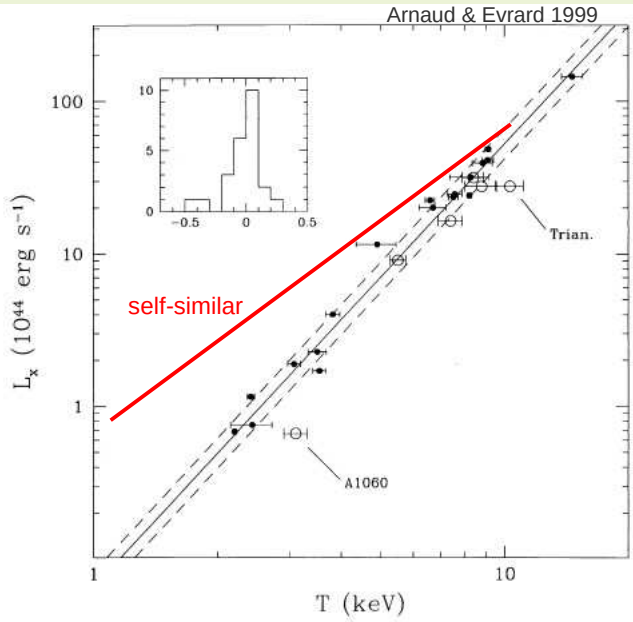

K-band stellar mass-temperature relation

Lin, Mohr, & Stanford 2004

$$\frac{L_{500}}{10^{12}\, h_{70}^{-2}\, L_\odot} = 3.95 \pm 0.11 \left(\frac{M_{500}}{2\times 10^{14}\, h_{70}^{-1}\, M_\odot}\right)^{0.69\pm 0.04}$$

~25% scatter in L_{500} at fixed T_X

assumes binding masses -

$$M_{500} = 2.55^{+0.29}_{-0.25} \times 10^{13} \frac{M_\odot}{h_{70}} \left(\frac{T_X}{1\ \mathrm{keV}}\right)^{1.58^{+0.06}_{-0.07}},$$

Finoguenov et al 2001

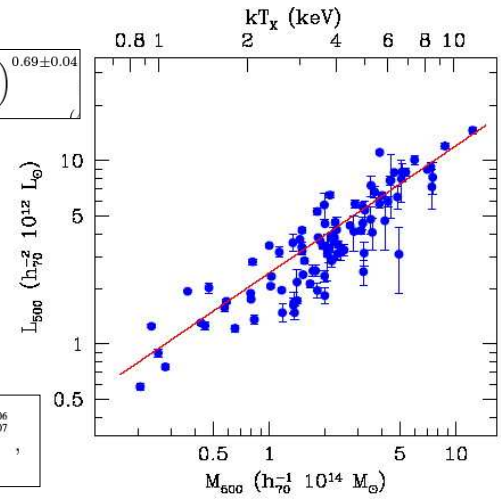

FIG. 3.— K-band luminosity–mass correlation within r_{500}. The best-fit relation has a slope of 0.69 ± 0.04. The scatter about the best-fit is 32%. For most of the clusters the uncertainties in light is smaller than the size of the points. For clarity we do not show the uncertainty in cluster mass (see Fig 5). At the top is the X–ray temperature, from which M_{500} is estimated (see Eqn 1).

halo occupation distribution

Lin, Mohr, & Stanford 2004

galaxy number ~ $M^{0.84\pm 0.04}$
nearly-Poisson variations

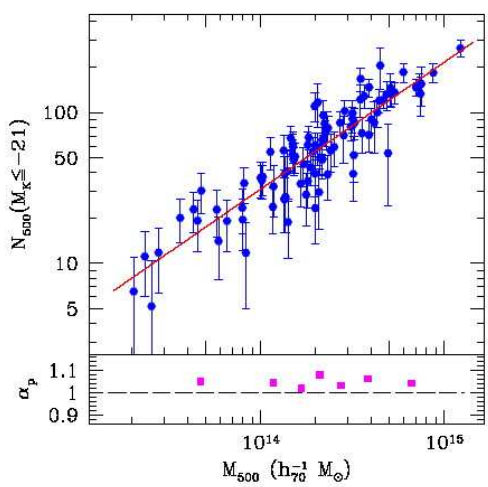

FIG. 6.— *Top*: Number of galaxies as a function of cluster mass. The best-fit relation gives $N \propto M^{0.84\pm 0.04}$. *Bottom*: deviation of the halo occupation number from a Poisson distribution. $\alpha_p = 1$ for Poisson, while a narrower (broader) distribution has $\alpha_p < 1 (> 1)$.

a promising outlook

space density | internal structure | scaling relations | spatial clustering

+ clusters (both real + virtual) display structural regularity
+ multiple mass components offer independent observables:
  - X-ray: T_X , L_X , $\Sigma_X(r)$
  - sub-mm: y_0 , $y(r)$
  - optical: N_{gal} , L_{gal} , $\Sigma_{gal}(r)$, σ_{gal} , lensing

  and several independent ways to infer mass:
  - T_X , σ_{gal} , $\int y$, clustering bias, lensing , ...
+ large (>10^4) samples (sub-mm + optical + X-ray) are upcoming
+ accuracy and fidelity of computational modeling are improving

clustering provides additional mass calibration

Lima & Hu 2004
Majumdar & Mohr 2003

SZ surveys can be *self-calibrating*
(or cross-calibrated with surveys at other wavelength)

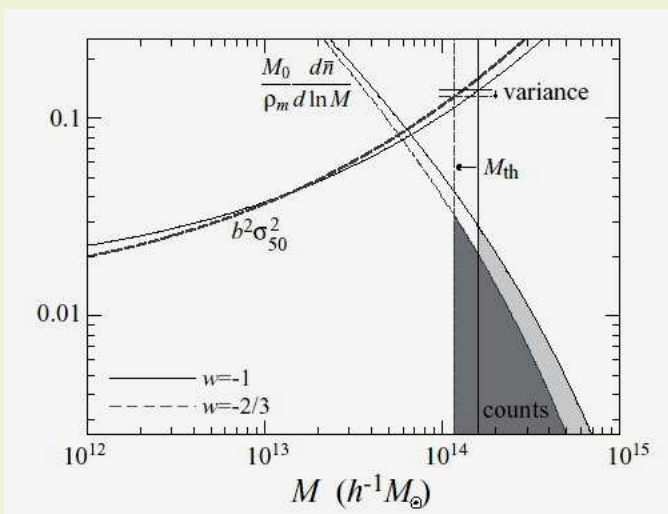

counts+clustering=powerful cosmological constraints

parameter forecasts for self-calibrated South Pole Telescope SZ survey

Lima & Hu 2004

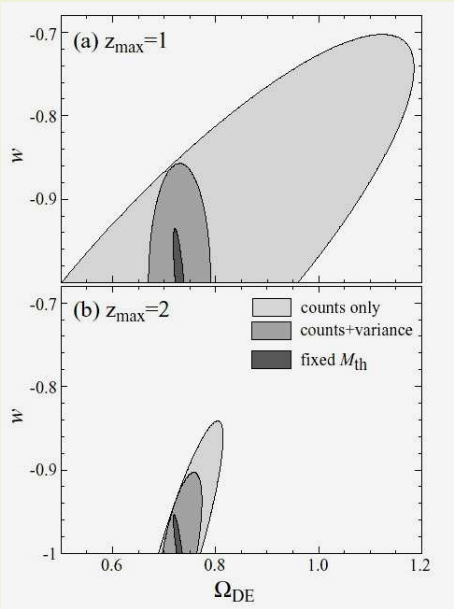

clusters as cosmological tools? need correct astrophysics!

$$P(\text{cosm} \mid \text{obs}) = P_{\text{prior}}(\text{cosm})\, P(\text{obs} \mid \text{cosm}) \,/\, P(\text{obs})$$

theoretical efforts & uncertainties lie here

first-order treatment: problem is separable

$$P(\text{obs} \mid \text{cosm}) \sim P(M,z \mid \text{cosm})\; P(\text{obs} \mid M,z)$$

- how many DM halos? $n\,(M,z \mid \text{cosm})$ **solved** (±10%)
- how do halos `light up'? $P\,(\text{obs} \mid M,z)$ **working on it** …

open issues…

– will photo-z's be sufficient?
– how do we best employ ALL the data on clusters? (VO+TVO?)
– is the connection between mass and observables too complex?
– can we correctly model sample selection biases?
– how `entangled' are astrophysical and cosmological parameters?
etc…